Journal of Materials Chemistry A

Accepted Manuscript

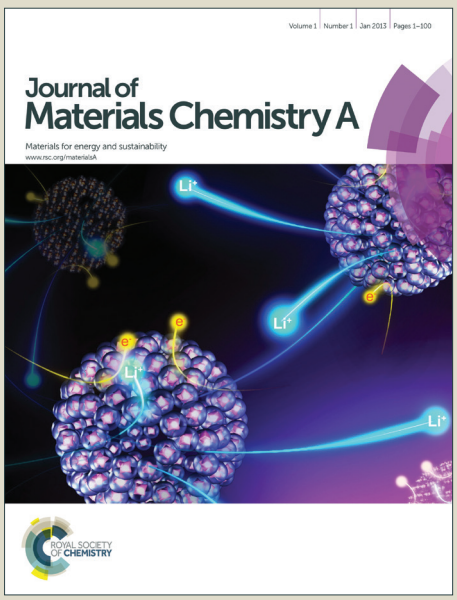

ROYAL SOCIETY OF CHEMISTRY

www.rsc.org/materialsA

Journal Name

RSCPublishing

ARTICLE

Porphyrinic porous organic frameworks: preparation and post-synthetic modification via demetallation-remetallation

Cite this: DOI: 10.1039/x0xx00000x

Received 00th January 2012,
Accepted 00th January 2012

DOI: 10.1039/x0xx00000x

www.rsc.org/

Qipu Lin,[a] Jingzhi Lu,[a] Zhaodi Yang,[a, b] Xiao Cheng Zeng[a] and Jian Zhang*[a]

We report a systematic synthesis of twelve porphyrinic porous organic frameworks (por-POF-***n***, ***n***=**1**-**12**) using building blocks with different sizes and connectivities, and we show that as the monomer's size and connectivity increase, the BET surface area and gas uptake capacity of the resulting por-POFs consistently increase, which suggests minimized network interpenetration. Importantly, we demonstrate that the metal center in por-POF-**8** can be modified through a post-synthetic demetallation-remetallation process, which provides an excellent opportunity to investigate the effect of the coordinatively unsaturated metal sites on gas adsorption. In particular, demetallated por-POF-**8**-2H and remetallated por-POF-**8**-FeCl and por-POF-**8**-Ni exhibit similar isosteric heats of adsorption (Q_{st}) toward H_2 and CO_2, which indicates that there is a limited effect of the porphyrin metal center on the gas uptake of por-POFs. This finding is further supported by a density-functional theory (DFT) calculation. The post-synthetically generated por-POF-**8**-FeCl shows an excellent biomimetic catalytic activity towards the oxidation of pyrogallol, demonstrating the great potentials of highly stable por-POFs as a new class of biomimetic catalysts.

Introduction

(Metallo)porphyrins are an important class of compounds that have unique photochemical, biochemical, electronic, optical, and catalytic properties.[1] In many cases, these properties are highly dependent on the assembly of multi-(metallo)porphyrin moieties.[2] Porphyrinic metal-organic frameworks (MOFs)[3] and covalent-organic frameworks (COFs)[4] are two examples of crystalline architectures that are composed of well-organized porphyrinic arrays, which are beneficial for structure-property investigations.[5] However, most porphyrinic MOFs and COFs have limited physicochemical stability, which is problematic for realizing their applications.[6] Furthermore, possible blocking of active porphyrin metal sites by axial coordinative ligands in MOFs[7] or the two-dimensional eclipsed close stacking in COFs[8] is undesirable for catalytic reactions where substrates require easy access to the active metal sites. Recently, porphyrinic porous organic frameworks (por-POFs) have emerged as a new generation of multi-porphyrin architectures.[9] As a subclass of porous organic polymers,[10] por-POFs are amorphous, three-dimensional networks constructed from inter-connected (metallo)porphyrins. Por-POFs exhibit not only outstanding thermal and physicochemical stability, but also comparable high surface area and pore volumes as porphyrinic MOFs and COFs,[11] good for a number of applications such as gas uptake,[12] sensing,[13] small molecule adsorption,[14] and others.[15] More importantly, most porphyrin active sites in por-POFs can be preserved and exposed,[16] making them extremely attractive for catalysis.[17]

A limiting factor for wide applications of porphyrinic materials, however, is the typical low yield synthesis of porphyrin macrocycles. Therefore, it is highly desirable to develop a strategy to reuse these materials via chemical modification of porphyrin macrocycles (i.e. the active metal centers), instead of resynthesis. This indeed is a viable approach since many interesting properties of metalloporphyrins are dictated by the coordinated metal ions. Porphyrins and metalloporphyrins, to some extent, can be interconverted through demetallation-remetallation,[18] which well serves the purpose of chemical modification. However, this procedure often requires harsh reaction condition like high temperature or acid treatment, and it has not been widely used in porphyrinic MOFs and COFs that have inferior physicochemical stability.[19] We hypothesize that this demetallation-remetallation process is suitable for post-synthetic modification of the active metal sites and, consequently, properties of por-POFs due to their outstanding thermal and physicochemical stability. Herein, we describe a systematic synthesis of twelve porphyrinic porous organic frameworks (por-POF-***n***, ***n*** = **1**-**12**) using Sonogashira-Hagihara coupling of two Zn-metallated porphyrinic alkynes with six

different aryl iodides. We then successfully utilized the demetallation-remetallation strategy and post-synthetically modified the active metal centers of por-POF-**8**. The applicability of this strategy was then demonstrated by a comparative gas adsorption study of free-base, Fe- and Ni-metallated por-POF-**8**-X (X = 2H, FeCl, and Ni) as well as a biomimetic study of por-POF-**8**-FeCl.

Results and discussion

Synthesis and characterization of por-POFs

Two Zn-metallated porphyrinic monomers with different size, 5,10,15,20-tetrakis(4-ethynyl)porphyrin-zinc (II) (**P1-Zn**) and 5,10,15,20-tetrakis(4-ethynylphenyl)porphyrin-zinc (II) (**P2-Zn**), synthesized in three steps from pyrrole with (trimethylsilyl)ethynyl-aldehyde and 4-(trimethylsilyl)ethynyl-benzaldehyde (Electronic Supplementary Information (ESI)), respectively, were reacted with six different aryl iodides of various sizes and connectivities using palladium-catalyzed Sonagashira-Hagihara coupling reactions (Scheme 1). A total number of twelve porous polymers (por-POF-***n***, ***n*=1-12**) were obtained in high yields. Since synthetic method and procedure significantly affect the porosity of resulting polymers,[20] we used the Brunauer-Emmett-Teller surface area (SA_{BET}) of por-POF-**7**, synthesized by the **P2-Zn**+**I3** polymerization reaction (Scheme 1), as the criterion to optimize polymerization conditions. Different solvents, temperatures, and monomer concentrations were studied (ESI). Based on SA_{BET} and adsorption capacity of N_2, H_2, and CO_2, we determined that the polymerization reaction was best conducted in a solution mixture of THF:Et_3N (v/v: 4:1) at 50 °C with a monomer concentration of 40 mM (ESI Figs. S1-S12). All por-POFs are insoluble in common organic solvents. The excellent efficiency of network formation was demonstrated by the typical high yield (after purification, >90%).

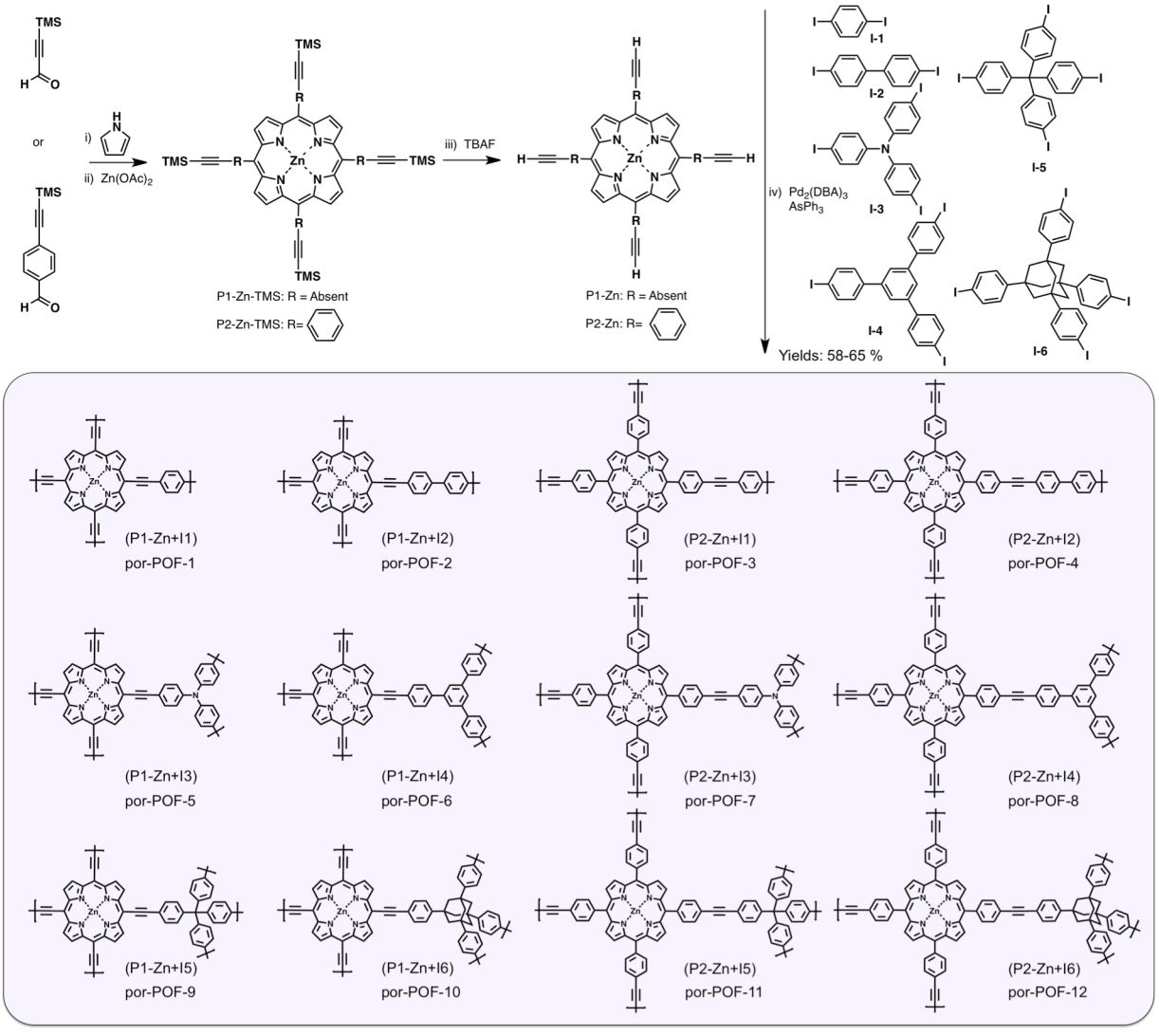

Scheme 1 Synthesis of por-POFs. Reaction conditions: (i) $BF_3{\cdot}OEt_2$, CH_2Cl_2, -78 °C, 6 h; 2,3-dichloro-5,6-dicyano-p-benzoquinone (DDQ), room temperature, 1 h. (ii) $Zn(OAc)_2$, $CHCl_3$-CH_3OH, reflux, overnight. (iii) tetrabutylammonium fluoride (TBAF), THF-CH_2Cl_2, room temperature, 1 h. (iv) $Pd_2(dba)_3$, $AsPh_3$, THF/Et_3N (v/v: 4:1), 50 °C, 72 h.

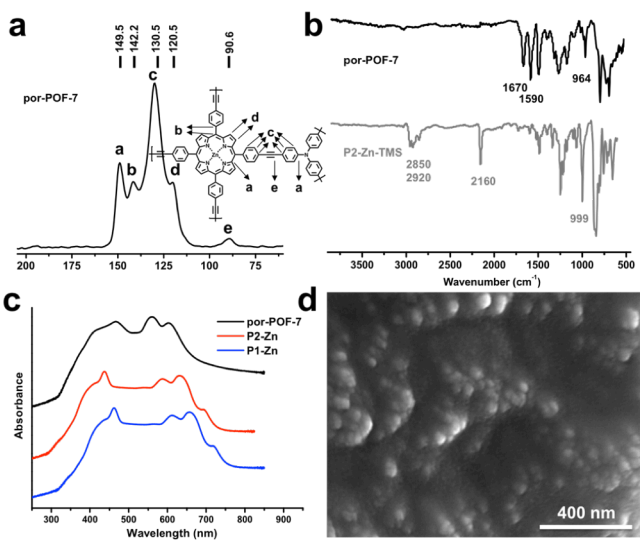

Fig. 1 (a) Solid-state CP/MAS ^{13}C NMR spectrum of por-POF-**7**. (b) FT-IR spectra of por-POF-**7** and **P2-Zn-TMS**. (c) UV-vis diffuse reflectance spectra of por-POF-**7**, monomer **P2-Zn** and **P1-Zn**. (d) SEM image of por-POF-**7**.

The structure of por-POFs was carefully characterized (ESI). Here, characterization of por-POF-**7** was used as an example of detailed description. Elemental analysis (C, H, and N) and ICP-MS analysis (Zn) of por-POF-**7** revealed that the C, H, N, and Zn contents are 76.18, 4.50, 6.53, and 4.21 wt%, respectively, which are lower than their corresponding theoretical values, possibly due to the presence of unreacted terminal iodo groups. Solid-state CP/MAS ^{13}C NMR spectrum (Fig. 1a) of por-POF-**7** shows four broad peaks at 149.5, 142.2, 130.5, and 120.5 ppm that are assigned to the phenylene moiety and porphyrin macrocycle. The weak resonance peak at 90.6 ppm is attributed to the acetylene group. Similar chemical shifts were obtained in the CP/MAS ^{13}C NMR spectra of other por-POFs (ESI Figs. S13-15). The N-H stretching in pyrrole (3314 cm^{-1}) disappears and the characteristic N-Zn in-plane bending at 964 cm^{-1} (close to that of **P2-Zn-TMS**: 999 cm^{-1}) appears in the FT-IR spectrum of por-POF-**7**, indicating the coordination of zinc (Fig. 1b).[21] Moreover, the absence of terminal alkyne's characteristic bands at ca. 2160 and 3300 cm^{-1} of **P2-Zn** (Fig. 1b) is indicative of a successful coupling reaction. The solid-state UV-vis diffuse reflectance spectrum of the por-POF-**7** shows the Soret band at 440 nm ($S_0 \rightarrow S_2$ absorption) and Q-bands at 550-600 nm ($S_0 \rightarrow S_1$ absorption), which are slightly red-shifted and blue-shifted, respectively, compared to the monomer **P2-Zn**, suggesting a highly conjugated nature of the polymer (Fig. 1c). Interestingly, compared to **P2-Zn**, all bands of **P1-Zn** are red-shifted as a result of the decreased energy gap of the frontier orbitals due to the expanded π-conjugation of the acetylene moiety in **P1-Zn** (Fig. 1c). The scanning electron microscopy (SEM) image shows that por-POF-**7** consists of uniform but highly aggregated particles with sizes ranging from 0.03-0.1 μm (Fig. 1d). Thermogravimetric analysis (TGA) shows por-POF-**7** is highly stable up to 400 °C under N_2 (Fig. S21).

Porosity measurements and gas storage studies

The porosity of por-POFs was examined using N_2 sorption measurement at 77 K (Fig. 2 and Fig. S22). At low pressure from 0-0.1 bar, uptake of N_2 increased rapidly, which strongly suggests that all por-POFs possess permanent micropores (Fig. S22). Like many other amorphous porous polymers, a hysteresis between adsorption and desorption is present and indicates that all POFs also contain mesopores and exhibit a pore-network effect (ESI Table S1).[22] We used a BET model in the pressure range of P/P_0 = 0.05−0.20 to calculate the SA_{BET} (Fig. 2). To our surprise, the SA_{BET} consistently increased as the size and connectivity of porphyrin monomers and aryl iodides increased. For example, por-POF-**12,** constructed with the longer porphyrin monomer **(P2-Zn)** and largest sized, four-connected iodide (**I6**), exhibits the highest SA_{BET} of 1379 $m^2 g^{-1}$ and a pore volume of 0.72 $cm^3 g^{-1}$. This linear correlation is in sharp contrast to many previous examples of porous polymers

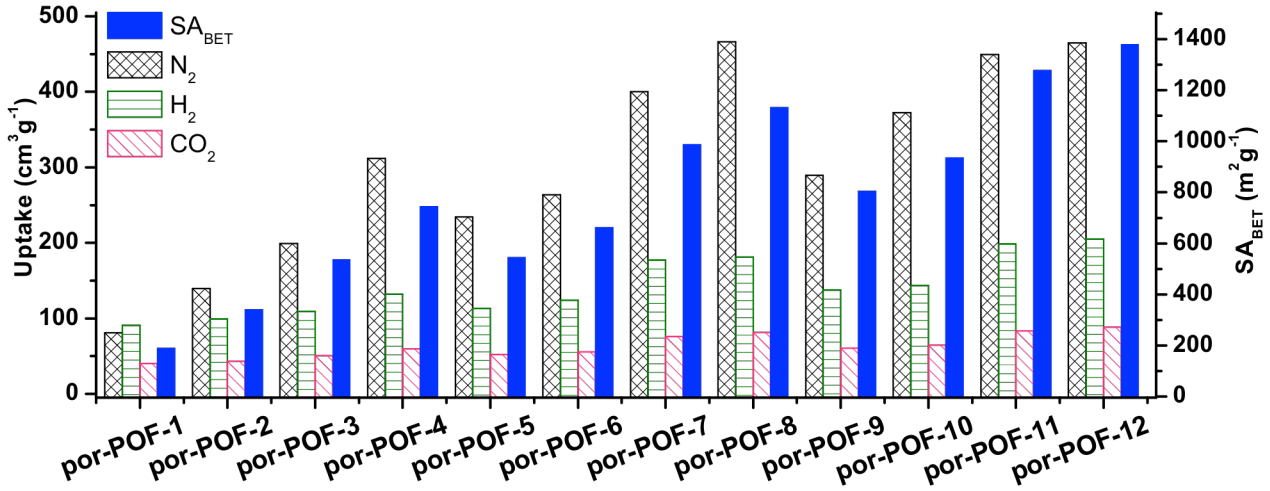

Fig. 2 SA_{BET} and gas uptake capacities of por-POFs.

that show decreased SA_{BET} as the monomer size increases because of interpenetration.[23] We attribute our unusual finding to the large size of porphyrin monomers, which can prevent the interpenetration of networks. Indeed, using bulky ligand in MOFs' synthesis is an effective strategy to prevent network interpenetration.[24] Further, uptake of H_2 at 77 K and CO_2 at 273 K was also determined (Fig. 2). All the N_2, H_2, and CO_2 sorption isotherms of por-POFs display increasing sorption capacity as monomers' sizes and connectivities increase, similar to the trend observed for SA_{BET} (Fig. 2 and ESI Table S1).

Demetallation-remetallation

Due to their highly covalently cross-linked networks, por-POFs can resist harsh reaction conditions in a post-synthetic demetallation-remetallation treatment, which can generate a wide range of porphyrinic materials with different metal centers. For example, after treating with concentrated HCl, por-POF-**8** was readily transformed into a metal-free porous polymer, por-POF-**8**-2H, which consists of free-base porphyrin moieties as confirmed by appearance of N-H stretching (3,320 cm^{-1}) in the FT-IR spectrum (Fig. S25). Subsequent reaction of por-POF-**8**-2H with $FeCl_2$ and $Ni(OAc)_2$ resulted in the formation of por-POF-**8**-FeCl and por-POF-**8**-Ni, respectively (see Experimental for detailed synthetic procedure). FT-IR analysis of the remetallated por-POFs reveals a significant decrease in the intensity of the N-H stretch, indicating the deprotonation of N-H bonds and the formation of M-N bonds (Fig. S25). ICP-MS analysis also confirms the successful remetallation of por-POF-**8**-2H with up to 2.7 wt% of Fe or 3.6 wt% of Ni, slightly lower than the theoretical metallation capacities based on the ideal stoichiometry of por-POF-**8**-X (4.7 and 5.0 wt% for X = FeCl and Ni, respectively), probably due to the presence of "dead space" where the porphyrin macrocycles are not accessible. Nevertheless, post-synthetic demetallation-remetallation treatment offers an alternate approach to chemically modify por-POFs without dissolution or degradation of the framework. The integrity of the covalently bonded structure and porosity after treating with concentrated HCl is largely remained, as evidenced by the similar SA_{BET} of por-POF-**8**-2H (991 m^2 g^{-1}) compared to that of por-POF-**8** (1114 m^2 g^{-1}) (Fig. S26).

Effect of metal site on gas uptake

As for MOFs, both theoretical calculations and experimental results have shown that coordinatively unsaturated metal sites can increase the initial isosteric heat of adsorption (Q_{st}) and overall adsorption capacity.[25] Metallated porphyrins also consist of coordinatively unsaturated metal sites upon the removal of the axial bonded solvent molecules. Thus, it is interesting to investigate the effect of porphyrin metal site on gas uptake. Recently, Yu *et al*. reported that a Fe-porphyrinic porous polymer, P(Fe-TTPP), exhibits a "finite increase" in H_2 adsorption,[12a] however, it is not clear if metallated porphyrin macrocycles can provide a strong binding environment for other adsorbates such as CO_2. Also, the impact of the identity of metal on gas adsorption is not currently available.

The efficient demetallation-remetallation process provides an opportunity to study the effect of porphyrin metal sites on gas uptake. As described above, demetallation of por-POF-**8** leads to the formation of free base porphyrinic por-POF-**8**-2H, which has a N_2 uptake of 466 cm^3 g^{-1} (STP) and a SA_{BET} and $SA_{Langmuir}$ surface area of 991 and 1578 m^2 g^{-1}, respectively. Por-POF-**8**-2H contains three types of pores with sizes of 0.8, 1.3 nm, and 2.3 nm, basing on the density functional theory (DFT) calculation from the N_2 adsorption measurement (Fig. S26). Introduction of FeCl and Ni at the porphyrin center slightly reduced the dominant pore size and the surface area (max. uptake = 362.5 and 408.7 cm^3 g^{-1}, $SA_{BET/Langmuir}$ = 814/1287 and 893/1414 m^2 g^{-1} for por-POF-**8**-FeCl and por-POF-**8**-Ni, respectively) (Fig. S26 and Table S3). Although the decrease of SA_{BET} after porphyrin metallation is not well understood, a similar finding was also reported for PTTPP and P(Fe-TTPP).[12a] Both por-POF-**8**-FeCl and por-POF-**8**-Ni show lower H_2 uptake than por-POF-**8**-2H (Fig. 3a), consistent with H_2 adsorption of PTTPP (free base) and P(Fe-TTPP):[12a] the excess adsorption capacity of H_2 (77 K, 1 bar) decreases from 175.7 (por-POF-**8**-**2**H) to 167.5 (por-POF-**8**-Ni) and 150.8 cm^3 g^{-1} (por-POF-**8**-FeCl). Isosteric heat of adsorption (Q_{st}) at zero coverage is a good indicator of the framework-gas interaction. Based on the H_2 sorption isotherms at 77 K and 87 K, we determined the Q_{st} of por-POF-**8**-2H, por-POF-**8**-FeCl, and por-POF-**8**-Ni to be 8.36, 8.11, and 8.44 kJ mol^{-1}, respectively, which further confirmed the limited impact of the porphyrinic metal site on the H_2 uptake at low pressure (< 1 bar). CO_2 adsorption isotherms were also measured. Por-POF-**8**-2H has a CO_2 uptake of 53.3 cm^3 g^{-1} at 273 K, slightly larger than that of

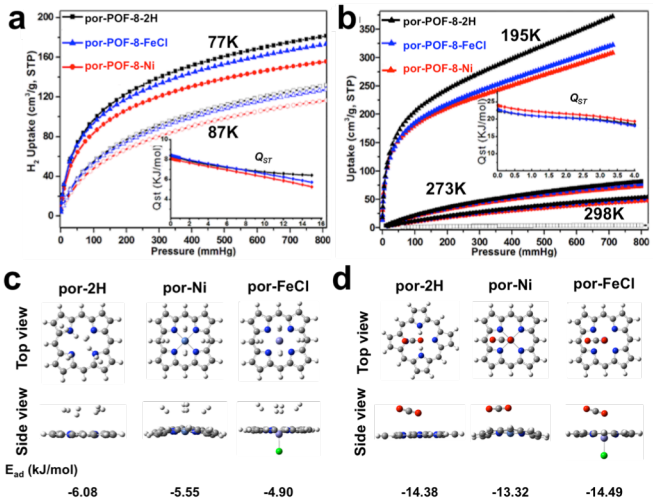

Fig. 3 (a) Measured H_2 adsorption isotherms at 77 and 87 K; the inset shows Q_{st} of H_2. (b) CO_2 uptake isotherm at 195, 273, and 298 K; the inset shows the Q_{st} for CO_2. (c, d) Optimized structures with four H_2 or one CO_2 molecule(s) adsorbed on (metallo)porphyrin. Adsorption energies are computed using the ωB97XD-/6-311G(d,p) level of theory.

por-POF-**8**-FeCl and por-POF-**8**-Ni (Fig. 3b). A similar trend was also observed at 298 K. However, a much-pronounced difference in CO_2 adsorption was present at 195 K (Fig. 3b): por-POF-**8**-2H exhibits a CO_2 uptake of 372.5 cm^3 g^{-1} at 0.93 bar, much higher than that of por-POF-**8**-Ni (322.0 cm^3 g^{-1}) and por-POF-**8**-FeCl (308.2 cm^3 g^{-1}), but still consistent with the trend of SA_{BET}. For CO_2 adsorption, por-POF-**8**-FeCl has an initial Q_{st} value of 24.0 kJ mol^{-1}, whereas por-POF-**8**-Ni and por-POF-**8**-2H have initial Q_{st} values of 22.8 and 22.5 kJ mol^{-1}, respectively. All values are similar to other nitrogen-rich porous organic frameworks.[23b, 26] Again, introducing Ni or Fe at the porphyrin cores has a limited effect on the heat of adsorption.

To further confirm the experimental results, we employed density-functional theory (DFT) methods using the Gaussian 09 package to calculate the binding energies. The wB97XD functional was chosen since it is considered as a suitable method for calculating weak interaction and it also includes empirical dispersion. To simplify the calculation, we only compared the H_2 and CO_2 adsorption ability on different porphyrin macrocycles (por-2H, por-Ni, and por-FeCl). As shown in Figs. S35-S36 (ESI), H_2 cannot be adsorbed vertically above the center of the porphyrin macrocycle. We have obtained the optimized geometries of four H_2 molecules adsorbed on one side of porphyrin macrocycle (Fig. 3c). However, only one CO_2 can be adsorbed on the porphyrin macrocycle based on the optimized geometry (Fig. 3d). The computed H_2 adsorption energies (using a dispersion-corrected DFT method at the level ωB97XD/6-311G(d,p)) are -6.08, -5.55, and -4.90 kJ mol^{-1} for por-2H, por-Ni, and por-FeCl respectively, and the difference among them is quite small (0.5-0.6 kJ mol^{-1}). Similarly, the computed adsorption energies at the same level of theory for CO_2 are almost same for por-2H and por-FeCl (-14.38 and -14.49 kJ mol^{-1}), and slightly stronger than that of the adsorption of CO_2 on por-Ni (-13.32 kJ mol^{-1}). These results indicate that the difference of Q_{st} induced by porphyrin metal center is indeed limited, and there is no obvious increase in adsorption energy for H_2 and CO_2 after the metalation with Ni and FeCl to porphyrin, consistent with our experimental results.

Biomimetic catalysis

Fe-porphyrin has excellent redox activities due to the presence of the active metal site similar to that of the heme complex in cytochrome P450, and it is often used in biomimetic catalytic reactions.[27] Using multi-porphyrin architectures for biomimetic studies is advantageous since they can effectively prevent the deactivation of the catalytic center caused by the formation peroxo-bridged Fe-porphyrin dimers during the oxidation reaction.[28] Por-POFs, in particular por-POF-**8** and por-POF-**12,** are constructed by large sized monomers, possessing accessible redox sites and ultrahigh stability in aqueous media and thus can serve as an ideal platform to study their biomimetic activities. Here, por-POF-**8**-FeCl, prepared through the demetallation-remetallation treatment of por-POF-**8** described above, was used as a prototypic porous polymer to characterize the biomimetic oxidation of pyrogallol, a reaction that is commonly used in standard assays to evaluate the catalytic performance of heme-like enzyme mimics (Fig. 4a).[29] Por-POF-**8**-2H and por-POF-**8**-Ni were also used as controls to demonstrate the importance of the Fe metal center in this catalytic reaction.

Before catalytic assays, the Fe content in por-POF-**8**-FeCl was measured to be 0.5 mmol g^{-1} by ICP-MS. We then studied a series of reactions that proceeded with different concentrations of pyrogallol (0.32 to 5.0 mM) in the presence of H_2O_2 (50 mM) and catalyst (5.0 μM active site equivalent). UV-vis absorption spectroscopy was used to monitor the formation of product (purpurogallin) at 420 nm (Fig. 4). The reaction proceeded very slowly with non-catalytic por-POF-**8**-2H or por-POF-**8**-Ni (Fig. 4b). However, faster reaction rates were observed when por-POF-**8**-FeCl is present. Curve fitting of the Michaelis−Menten plot generates two important parameters k_{cat} and K_m (Michaelis constant) (Fig. 4c). The k_{cat} indicates the maximum number of substrates being converted to product molecules under the optimal condition, while K_m represents the binding affinity of the catalyst for the substrate. Based on the curve fitting analysis, por-POF-**8**-FeCl shows a k_{cat} value of 5.48 min^{-1}, which is higher than that of other heterogeneous catalyst CEF-1 (0.33 min^{-1})[17d] and homogeneous catalyst hemin (2.4 min^{-1}),[29] but smaller than a recently reported MOF biomimetic catalyst PCN-222(Fe) (16.1 min^{-1}) (Table 1).[30] This is reasonable since PCN-222(Fe) contains channel-like mesopores with a diameter of 3.7 nm,[30] allowing faster diffusion that leads to a higher k_{cat}. On the contrary, por-POF-**8**-FeCl consists of both micropores and mesopores and, consequently, leads to a slower diffusion rate and a lower k_{cat}. Similar to PCN-222(Fe), por-POF-**8**-FeCl shows a stronger affinity to pyrogallol (K_m = 0.46 mM) than that of the natural horseradish peroxidase (HRP) (K_m = 0.81 mM) (Table 1). As for the overall catalytic performance, por-POF-**8**-FeCl exhibits

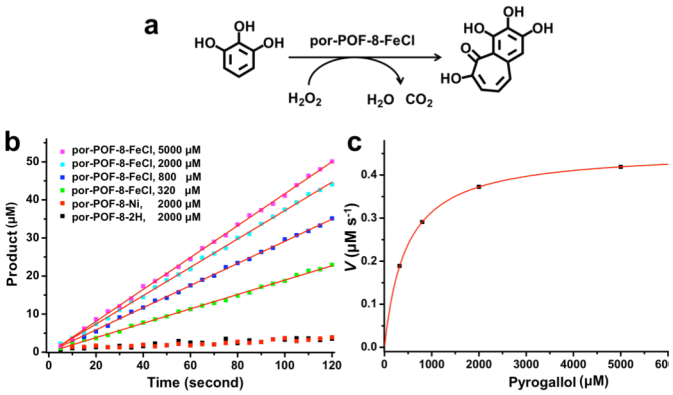

Fig. 4 (a) Reaction scheme of oxidation of pyrogallol. (b) Kinetic traces for oxidation of pyrogallol using H_2O_2 catalyzed by different por-POF-**8** based polymers. (c) Michaelis-Menten plot of the pyrogallol oxidation catalyzed by por-POF-8-FeCl, based on the oxidation rates obtained from Fig. 4a.

an efficiency (k_{cat}/K_m) of 1.20 × 10^4 M^{-1} min^{-1}, which is comparable to that of CEF-1 (8.26 × 10^4 M^{-1} min^{-1}) and PCN-222(Fe) (4.85 × 10^4 M^{-1} min^{-1}). The slightly lower catalytic efficiency of por-POF-**8**-FeCl might be due to the lack of additional pre-treatment such as ball milling with $BaSO_4$ to increase its wettability and hydrophilicity in aqueous solution, as what was performed for CEF-1.[17d]

Table 1 Kinetic parameters for the oxidation of pyrogallol by different catalysts

	k_{cat} (min^{-1})	K_m (mM)	k_{cat}/K_m (M^{-1} min^{-1})
por-POF-**8**-FeCl	5.48	0.46	1.20 × 10^4
CEF-1[17d]	0.33	0.0040	8.25 × 10^4
PCN-222(Fe)[30]	16.1	0.33	4.88 × 10^4
hemin[29]	2.4	NA	NA
HRP[29]	1.8 × 10^3	0.81	2.22 × 10^6

Conclusions

In summary, a series of robust porphyrinic porous organic frameworks (por-POFs) were synthesized using Sonogashira-Hagihara coupling reactions. The sizes and connectivities of the porphyrin and aryl iodide monomers dictate the porosity parameters of the resulting polymers: as the monomers' sizes and connectivities increase, the BET surface area and gas uptake capacity increase. We show that the metal center in por-POFs can be modified through post-synthetic demetallation-remetallation, which provides an opportunity to investigate the effect of the coordinatively unsaturated metal sites on gas adsorption. In particular, demetallated por-POF-**8**-2H and remetallated por-POF-**8**-FeCl and por-POF-**8**-Ni exhibit similar Q_{st} values for H_2 and CO_2, indicating the metal center has a limited impact on tuning the gas uptake capacity of porphyrinic porous materials. This finding is further supported by a wB97XD/6-311g** DFT calculation. In addition, post-synthetically generated por-POF-**8**-FeCl shows an excellent biomimetic catalytic activity towards the oxidation of pyrogallol, demonstrating the great potentials of highly stable por-POFs as a new class of biomimetic catalysts.

Experimental

Materials

All reagents, except the monomers **P1-Zn**, **P2-Zn**, **I5**, and **I6**, were obtained from commercial suppliers. Organic solvents such as THF, Et_3N, *N*,*N*-dimethylformamide (DMF), *N*-methyl-2-pyrrolidone (NMP), and dioxane were distilled over appropriate drying reagents under argon or obtained as anhydrous reagents from commercial sources without further purification.

Measurements

Solution ^1H NMR spectra were recorded on a Bruker FT-NMR spectrometer (400 MHz). Solid-state CP/MAS ^{13}C NMR spectra were recorded on a Bruker Avance III three-channel spectrometer, acquired using CP-TOSS pulse sequences, which are cross polarized and suppresses the spinning side bands. Mass spectra were recorded with the Applied Biosystem's Voyager DE-Pro MALDI-TOF mass spectrometer. Solid-state UV-Vis diffuse reflectance spectra were recorded on an Agilent Cary 300 UV-Vis spectrophotometer. Fourier transform infrared spectroscopy was performed on a Nicolet 380 FT-IR spectrometer. Elemental analysis (EA) was carried out with a Perkin-Elmer 2400 CHN Elemental Analyzer (Atlantic Microlab, Inc.). The thermogravimetric analysis was carried out using a TA Instruments SDT Q600 apparatus in the temperature range of 30 ^oC to 900 ^oC under air flow at a heating rate of 10 ^oC min^{-1}. Gas sorption measurements were carried out on a Micromeritics ASAP 2020 Physisorption Analyzer. Zn, Ni, and Fe contents were measured by Agilent inductively coupled plasma mass spectrometer (ICP-MS) 7500cx with the autosampler. Scanning electron microscopy (SEM) images were taken on Hitachi S4700 field-emission scanning electron microscope (FE-SEM).

Preparation of por-POF-1 (P1-Zn+I1)

In 250 mL flask, 5,10,15,20-tetrakis(4-ethynyl)porphyrin-zinc (II) (**P1-Zn**, 0.09 g, 0.2 mmol), 1,4-diiodobenzene (**I1**, 0.07 g, 0.2 mmol), and triphenylarsine ($AsPh_3$, 0.12 g, 0.4 mmol) were dissolved in a solvent mixture of anhydrous THF:Et_3N (80 mL:20 mL). The solution was degased before the catalyst tris(dibenzylidene-acetone)dipalladium(0) ($Pd_2(dba)_3$, 0.013 g, 0.01 mmol) was added. The reaction temperature was kept at 50 °C and stirred for 72 h. After cooled to room temperature, HCl (1M, 50 mL) was added and the reaction mixture was stirred for another 5 h to remove the residual salt. The precipitate was filtered and washed with water, THF, DMF, CH_2Cl_2, acetone, and methanol, followed by successive Soxhlet extraction with THF, CH_2Cl_2, and methanol. The obtained dark purple powder was further dried at 100 °C in oven for 24 h to give the final product.

All other por-POFs were synthesized via the similar procedure by polymerizing porphyrin monomers (**P1-Zn** or **P2-Zn**, 0.2 mmol) with corresponding aryl iodide (**I1**, **I2**, **I3**, **I4**, **I5**, or **I6**, 0.2 mmol) catalyzed by $Pd_2(dba)_3/AsPh_3$ in the solvent of THF:Et_3N (80 mL:20 mL) under Ar.

Preparation of por-POF-8-X (X = 2H, FeCl, and Ni)

Por-POF-**8** was immersed in aqueous HCl (6 M, 100 mL) and heated at 80 °C for 6 h, and the reaction mixture was subsequently filtered and washed with water, THF, and acetone, respectively, and isolated as por-POF-**8**-2H. Remetallation of por-POF-**8**-2H proceeded in DMF (100 mL) under reflux in the presence of $FeCl_2·4H_2O$ (2.5 g, 12.8 mmol) or $NiCl_2·6H_2O$ (3.1 g, 12.8 mmol) for 6 h. After the mixture was cooled to room temperature, water (150 mL) was added. The resultant metallated por-POF-**8**-X (X = FeCl and Ni) was filtered and purified by Soxhlet extraction with water, THF, and methanol.

Biomimetic oxidation kinetic study

The concentration of pyrogallol varies from 320-5000 μM with a fixed concentration of por-POF-**8**-FeCl catalyst (5.0 μM active site equivalent) and a H_2O_2 concentration of 50 mM. The catalytic reactions were monitored in kinetic mode at 420 nm (ε = 2.64 mM^{-1} cm^{-1}) with a Cary-300 UV-Vis spectrometer.

Acknowledgements

This work is supported by the University of Nebraska-Lincoln and Nebraska Center for Energy Sciences Research and UNL Holland Computing Center. J. Z. acknowledges the Donors of the American Chemical Society Petroleum Research Fund for partial support of this research. We are grateful to Dr. Dewey Barich for assistance in solid state CP/MAS ^{13}C NMR measurements.

Notes and references

[a] Department of Chemistry, University of Nebraska-Lincoln, Lincoln, Nebraska 68588, USA. E-mail: jzhang3@unl.edu; Fax: +1-402-272-9402; Tel: +1-402-272-2603

[b] College of Chemical and Environmental Engineering, Harbin University of Science and Technology, Harbin 150040, China

† Electronic Supplementary Information (ESI) available: Gas sorption study, synthesis of monomers, optimization of reaction conditions, characterizations of por-POFs, and computational analysis of binding energies. See DOI: 10.1039/b000000x/

1. M. O. Senge, in *The porphyrin handbook*, Academic Press, Boston, 2000, vol. 1, pp. 239.
2. (a) H. E. Toma and K. Araki, *Coord. Chem. Rev.*, 2000, **196**, 307; (b) C. M. Drain, A. Varotto and I. Radivojevic, *Chem. Rev.*, 2009, **109**, 1630; (c) I. Beletskaya, V. S. Tyurin, A. Y. Tsivadze, R. Guilard and C. Stern, *Chem. Rev.*, 2009, **109**, 1659.
3. (a) M. Zhao, S. Ou and C. D. Wu, *Acc. Chem. Res.*, 2014, **47**, 1199; (b) W. Y. Gao, M. Chrzanowski and S. Ma, *Chem. Soc. Rev.*, 2014; (c) J. A. Johnson, Q. Lin, L. C. Wu, N. Obaidi, Z. L. Olson, T. C. Reeson, Y. S. Chen and J. Zhang, *Chem. Commun.*, 2013, **49**, 2828.
4. (a) S. Wan, F. Gándara, A. Asano, H. Furukawa, A. Saeki, S. K. Dey, L. Liao, M. W. Ambrogio, Y. Y. Botros, X. Duan, S. Seki, J. F. Stoddart and O. M. Yaghi, *Chem. Mater.*, 2011, **23**, 4094; (b) X. Feng, L. Liu, Y. Honsho, A. Saeki, S. Seki, S. Irle, Y. Dong, A. Nagai and D. Jiang, *Angew. Chem., Int. Ed.*, 2012, **51**, 2618; (c) S. Kandambeth, D. B. Shinde, M. K. Panda, B. Lukose, T. Heine and R. Banerjee, *Angew. Chem., Int. Ed.*, 2013, **52**, 13052; (d) A. Nagai, X. Chen, X. Feng, X. Ding, Z. Guo and D. Jiang, *Angew. Chem., Int. Ed.*, 2013, **52**, 3770.
5. X. Chen, M. Addicoat, S. Irle, A. Nagai and D. Jiang, *J. Am. Chem. Soc.*, 2013, **135**, 546.
6. (a) P. M. Barron, C. A. Wray, C. Hu, Z. Guo and W. Choe, *Inorg. Chem.*, 2010, **49**, 10217; (b) X. Feng, L. Chen, Y. Dong and D. Jiang, *Chem. Commun.*, 2011, **47**, 1979.
7. E. Y. Choi, P. M. Barron, R. W. Novotny, H. T. Son, C. Hu and W. Choe, *Inorg. Chem.*, 2009, **48**, 426.
8. H. Xu, X. Chen, J. Gao, J. Lin, M. Addicoat, S. Irle and D. Jiang, *Chem. Commun.*, 2014, **50**, 1292.
9. N. B. McKeown, S. Hanif, K. Msayib, C. E. Tattershall and P. M. Budd, *Chem. Commun.*, 2002, 2782.
10. (a) D. Wu, F. Xu, B. Sun, R. Fu, H. He and K. Matyjaszewski, *Chem. Rev.*, 2012, **112**, 3959; (b) R. Dawson, A. I. Cooper and D. J. Adams, *Prog. Polym. Sci.*, 2012, **37**, 530; (c) Y. Xu, S. Jin, H. Xu, A. Nagai and D. Jiang, *Chem. Soc. Rev.*, 2013, **42**, 8012; (d) X. Zou, H. Ren and G. Zhu, *Chem. Commun.*, 2013, **49**, 3925; (e) Y. Jin, Y. Zhu and W. Zhang, *CrystEngComm*, 2013, **15**, 1484.
11. H. J. Mackintosh, P. M. Budd and N. B. McKeown, *J. Mater. Chem.*, 2008, **18**, 573.
12. (a) J. Xia, S. Yuan, Z. Wang, S. Kirklin, B. Dorney, D.-J. Liu and L. Yu, *Macromolecules*, 2010, **43**, 3325; (b) Z. Wang, S. Yuan, A. Mason, B. Reprogle, D.-J. Liu and L. Yu, *Macromolecules*, 2012, **45**, 7413; (c) A. Modak, M. Nandi, J. Mondal and A. Bhaumik, *Chem. Commun.*, 2012, **48**, 248.
13. K. Wu, J. Guo and C. Wang, *Chem. Commun.*, 2014, **50**, 695.
14. (a) X. S. Wang, J. Liu, J. M. Bonefont, D. Q. Yuan, P. K. Thallapally and S. Ma, *Chem. Commun.*, 2013, **49**, 1533; (b) X. Liu, Y. Xu, Z. Guo, A. Nagai and D. Jiang, *Chem. Commun.*, 2013, **49**, 3233.
15. (a) S. Yuan, J. L. Shui, L. Grabstanowicz, C. Chen, S. Commet, B. Reprogle, T. Xu, L. Yu and D. J. Liu, *Angew. Chem., Int. Ed.*, 2013, **52**, 8349; (b) A. Kong, B. Dong, X. Zhu, Y. Kong, J. Zhang and Y. Shan, *Chem.-Eur. J.*, 2013, **19**, 16170; (c) Z. Xiang, Y. Xue, D. Cao, L. Huang, J. F. Chen and L. Dai, *Angew. Chem., Int. Ed.*, 2014, **53**, 2433; (d) Z. S. Wu, L. Chen, J. Liu, K. Parvez, H. Liang, J. Shu, H. Sachdev, R. Graf, X. Feng and K. Mullen, *Adv. Mater.*, 2014, **26**, 1450.
16. R. K. Totten, Y. S. Kim, M. H. Weston, O. K. Farha, J. T. Hupp and S. T. Nguyen, *J. Am. Chem. Soc.*, 2013, **135**, 11720.
17. (a) L. Chen, Y. Yang and D. Jiang, *J. Am. Chem. Soc.*, 2010, **132**, 9138; (b) A. M. Shultz, O. K. Farha, J. T. Hupp and S. T. Nguyen, *Chem. Sci.*, 2011, **2**, 686; (c) L. Chen, Y. Yang, Z. Guo and D. Jiang, *Adv Mater*, 2011, **23**, 3149; (d) X.-S. Wang, M. Chrzanowski, D. Yuan, B. S. Sweeting and S. Ma, *Chem. Mater.*, 2014, **26**, 1639; (e) L.-J. Feng, Q. Chen, J.-H. Zhu, D.-P. Liu, Y.-C. Zhao and B.-H. Han, *Poly. Chem.*, 2014, **5**, 3081.
18. (a) P. Hambright and E. B. Fleisher, *Inorg. Chem.*, 1970, **9**, 1757; (b) D. K. Lavallee, *Comments Inorg. Chem.*, 1986, **5**, 155; (c) M. Linke, J.-C. Chambron, V. Heitz, J.-P. Sauvage and V. Semetey, *Chem. Commun.*, 1998, 2469; (d) K. Murakami, Y. Yamamoto, H. Yorimitsu and A. Osuka, *Chem.-Eur. J.*, 2013, **19**, 9123.
19. X. S. Wang, M. Chrzanowski, L. Wojtas, Y. S. Chen and S. Ma, *Chem.-Eur. J.*, 2013, **19**, 3297.
20. R. Dawson, A. Laybourn, Y. Z. Khimyak, D. J. Adams and A. I. Cooper, *Macromolecules*, 2010, **43**, 8524.
21. H. Ogoshi, *J. Chem. Phys.*, 1972, **57**, 4194.
22. (a) J. Jeromenok and J. Weber, *Langmuir*, 2013, **29**, 12982; (b) P. M. Budd, E. S. Elabas, B. S. Ghanem, S. Makhseed, N. B. McKeown, K. J. Msayib, C. E. Tattershall and D. Wang, *Adv. Mater.*, 2004, **16**, 456.
23. (a) W. Lu, D. Yuan, D. Zhao, C. I. Schilling, O. Plietzsch, T. Muller, S. Bräse, J. Guenther, J. Blümel, R. Krishna, Z. Li and H.-C. Zhou, *Chem. Mater.*, 2010, **22**, 5964; (b) Y. Zhu, H. Long and W. Zhang, *Chem. Mater.*, 2013, **25**, 1630; (c) J. X. Jiang, F. Su, A. Trewin, C. D. Wood, N. L. Campbell, H. Niu, C. Dickinson, A. Y. Ganin, M. J.

Rosseinsky, Y. Z. Khimyak and A. I. Cooper, *Angew. Chem., Int. Ed.*, 2007, **46**, 8574.
24. R. K. Deshpande, G. I. Waterhouse, G. B. Jameson and S. G. Telfer, *Chem. Commun.*, 2012, **48**, 1574.
25. (a) B. Chen, N. W. Ockwig, A. R. Millward, D. S. Contreras and O. M. Yaghi, *Angew. Chem., Int. Ed.*, 2005, **44**, 4745; (b) A. O. Yazaydin, R. Q. Snurr, T. H. Park, K. Koh, J. Liu, M. D. Levan, A. I. Benin, P. Jakubczak, M. Lanuza, D. B. Galloway, J. J. Low and R. R. Willis, *J. Am. Chem. Soc.*, 2009, **131**, 18198.
26. (a) H. A. Patel, S. H. Je, J. Park, D. P. Chen, Y. Jung, C. T. Yavuz and A. Coskun, *Nat. Commun.*, 2013, **4**, 1357; (b) M. R. Liebl and J. Senker, *Chem. Mater.*, 2013, **25**, 970; (c) W.-C. Song, X.-K. Xu, Q. Chen, Z.-Z. Zhuang and X.-H. Bu, *Poly. Chem.*, 2013, **4**, 4690; (d) G. Li and Z. Wang, *Macromolecules*, 2013, **46**, 3058.
27. I. Tabushi, *Coord. Chem. Rev.*, 1988, **86**, 1.
28. M. C. Feiters, A. E. Rowan and R. J. M. Nolte, *Chem. Soc. Rev.*, 2000, **29**, 375.
29. Q. Wang, Z. Yang, X. Zhang, X. Xiao, C. K. Chang and B. Xu, *Angew. Chem., Int. Ed.*, 2007, **46**, 4285.
30. D. Feng, Z. Y. Gu, J. R. Li, H. L. Jiang, Z. Wei and H. C. Zhou, *Angew. Chem., Int. Ed.*, 2012, **51**, 10307.